Adaptive Channel Equalization for Turbid Underwater Optical Communication

Kaitlin Dunn, *Student Member, IEEE,* Luke Rumbaugh, *Member, IEEE* Mahesh Banavar, *Senior Member, IEEE* Brandon Cochenour, *Senior Member, IEEE* and William Jemison, *Fellow, IEEE*

***Abstract*—Experimental measurements have been performed to evaluate the effect of multipath scattering on the performance of underwater optical communication links. A simple channel model based on the data collected in these measurements is proposed whose three parameters can be determined adaptively over a wide range of turbidities without using *a priori* information. These channel models are then used to construct channel equalizers. On-off keyed links with and without channel equalization were then simulated. Assuming a 20 dB signal-to-noise ratio, channel equalization allows a 1.1 Gbps link to be closed up to 14 attenuation lengths with a bit-error-ratio (BER) of 10^{-6} (versus 12 attenuation lengths without equalization). By reducing the data rate to 275 Mbps, channel equalization extends link closure out to 28 attenuation lengths with a BER of $10^{-3.5}$ (versus 20 attenuation lengths without equalization).**

I. Introduction

High speed, free space optical communication underwater provides advantages for applications with unmanned and autonomous underwater vehicles or underwater sensor networks [2], [3], [1]. However, data fidelity in optical links is highly dependent on the inherent optical properties of the specific ocean environment. Beer's Law, given by $P(c,d) = P_o \exp(-cd)$, provides a first order description of optical attenuation underwater, where P is the received power, P_0 is the transmitted power, c is the attenuation coefficient (m^{-1}), and d is the propagation distance in meters. The attenuation coefficient characterizes the loss due to absorption and scattering in the channel, and the dimensionless product cd is referred to as the attenuation length. Though computationally convenient, Beer's Law is insufficient for describing the contribution of scattered light at the optical receiver. This contribution is inevitable at long ranges, high turbidities, or with realistic receiver apertures and angular fields-of-view. Additionally, Beer's Law is time independent, meaning it provides no information about how the collection of scattered light increases inter-symbol interference (ISI) and decreases channel capacity.

To determine the effect that scattered light has on temporal dispersion in free space underwater optical channels, numerical or analytic modeling of the Radiative Transfer Equation is required. Experimental data to validate these models has been reported, but contained information about the magnitude response of the channel only [4], [5]. Most recently, Cochenour *et al.* measured for the first time *both* the magnitude and the phase response [6] of turbid underwater optical channels in the laboratory. In the context of underwater optical communication links, the description of both the magnitude and phase response of the channel allows for the development and application of channel equalization filters to counteract the temporal dispersion arising from the collection of multiply scattered light. While channel equalization has been previously considered for underwater wireless optical communication ([1], [7]), those studies only compensated for temporal deficiencies of the laser source and receiver. It did not consider the temporal dispersion of the actual propagation medium.

This paper illustrates the benefits of channel equalization to compensate for the ISI that arises due to multiple scattering of the optical signal through the underwater channel. Using the experimental channel measurements from [6], the underwater wireless optical channel is simply modeled as a 3-parameter infinite impulse response (IIR) digital filter. These parameters can be determined adaptively without any *a priori* knowledge of the channel. The adaptively determined channel models are then inverted to provide channel equalization. Simulations show that channel equalizers are effective at improving error-performance and extending operation to longer attenuation lengths.

II. Channel Model and Equalization

A. Experimental Channel Response Measurements

An optical data stream after propagation through an underwater channel can be described by,

$$d(n) = x(n) * h(n) + n_0 \tag{1}$$

where $d(n)$ is the received data sequence, $x(n)$ is the transmitted data sequence, $h(n)$ is the discrete-time channel impulse response, and n_0 is additive white Gaussian noise (AWGN) with variance $\sigma(n)$. The channel impulse response, $h(n)$, has the Fourier Transform $H(e^{j\Omega}) = M(\Omega)e^{j\Phi(\Omega)}$ where $M(\Omega))$ and $\Phi(\Omega)$ are the magnitude and phase responses respectively.

Experimental measurements of $H(e^{j\Omega})$ were performed in [6]. A network analyzer was used to modulate a 532 nm laser transmitter whose beam passed through a 3.56 m long water tank before being detected by a photomultiplier tube with an 0.0508 m aperture and 9 degree field-of-view (full angle). The network analyzer measured the magnitude and

K. Dunn is with the Department of Optics, University of Rochester, Rochester, NY USA.

L. Rumbaugh, M. Banavar, and W. Jemison are with the Department of Electrical and Computer Engineering, Clarkson University, Potsdam, NY 13699 USA e-mail: rumbaugh@clarkson.edu.

B. Cochenour is with the Naval Air Warfare Center Aircraft Division, Electro-Optics and Special Mission Sensors Division, Patuxent River, MD.

Manuscript submitted October 10, 2017.

phase of the received signal relative to the signal used to modulate the source. Measurements were obtained at modulation frequencies from 0.1 to 1.1 GHz in 0.1 GHz steps, over a wide range of turbidities, and for various scattering particles. This work considers the experimentally measured channel responses where 930 nm diameter polystyrene beads were used as the scattering agent.

The channel impulse response, $h(n)$, at each turbidity can be formed by performing the inverse Fast Fourier Transform (IFFT) of the experimentally measured complex frequency responses, $H(e^{j\Omega})$. To increase resolution in the time domain impulse response, the frequency responses were zero-padded by a factor of 16 prior to taking the IFFT. An anti-imaging filter was applied after the IFFT [9]. The resultant time domain channel impulse responses had an effective sampling rate f_s of 2.2 GSPS, a sample interval t_s of 0.45 ns, and a duration of 10 ns.

The resultant channel impulse responses, derived from the experimentally measured frequency domain responses, are shown in Fig. 1. The impulse responses evolve logically with increasing attenuation length. For $cd < 10$ (Fig. 1, left) the peak of $h(n)$ is located at zero delay indicating that non-scattered light (which would experience no excess path delay beyond the direct path between transmitter and receiver) and single-scattered light (which experiences a path delay much less than t_s) dominate the received signal. For $10 < cd < 15$ (Fig. 1, center) the response exhibits a "tail" due to the spread of photon arrival times that are attributed to a rising multiply scattered component. For $cd > 15$ (Fig. 1, right), the impulse response is dominated by multiply scattered light as evidenced by both a delay in the maximum amplitude of the response as well as a widening spread. These trends versus attenuation length are consistent with the analysis in [6].

The results of Fig. 1 can be summarized by the following observations that are key to this work's novelty:

1. The experimentally measured impulse responses $h(n) \leftrightarrow H(e^{j\Omega})$ evolve in a logical and well-behaved fashion with increasing turbidity. Namely, an increase in multiple scattering results in both a temporal broadening and delay of the optical pulse.

2. The logical evolution the actual measured impulse responses, $h(n) \leftrightarrow H(e^{j\Omega})$, with increasing turbidity suggests that the channel may be easily modeled as $\hat{h}(n) \leftrightarrow \hat{H}(z)$ using a simple digital filter structure of only a few parameters.

3. The simplicity of the proposed filter model should allow for the filter parameters to be discovered adaptively using a training sequence and no *a priori* knowledge.

4. The adaptively determined channel estimate can be inverted to obtain an appropriate channel equalization filter, which can be included at the receiver of a communications system to mitigate the effects of multiple scattering and thus increase the achievable data rate, range, or error performance of the system.

These ideas are explored below and are demonstrated in proof-of-concept simulations.

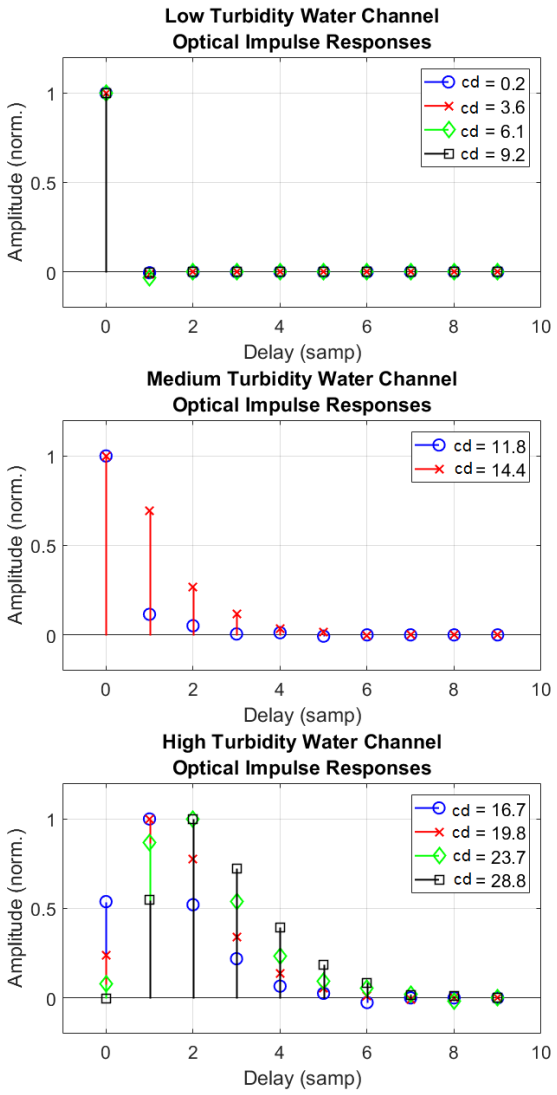

Fig. 1. The channel impulse responses $h(n)$ seen by the modulated laser beam, obtained from the channel frequency responses $H(e^{j\Omega})$ as experimentally measured in [6]. Here, *cd* is the number of attenuation lengths the light passed through.

B. Channel Response Model

The channel model must accurately describe the experimentally measured channel responses, while also being invertible to allow channel equalization. Physically, we understand the channel as a linear addition of multipath components, i.e. as a finite impulse response (FIR) system. However, in order to facilitate inversion, we model the channel as an infinite impulse response (IIR) filter whose frequency response approximates $H(e^{j\Omega})$. This IIR filter model's z-domain expression is

$$\hat{H}(z) = \frac{b_0 + b_1 z^{-1} + ... + b_L z^{-L}}{1 - a_1 z^{-1}} \tag{2}$$

It is implied that each parameter is inherently a function of system parameters, link range/geometry, and water optical properties. While no one set of parameter values can represent all combinations of said variables, the filter parameters can be understood physically in general by visualizing how a short

optical pulse is temporally dispersed upon traveling through a turbid channel. The parameter b_0 represents the amplitude of the zero-delay term of $h(n)$, where 'delay' is defined as the delay in excess of the direct path between transmitter and receiver. Thus, the zero-delay term physically embodies the non-scattered component as well as any minimally scattered light with delay $< t_s$. The parameter L represents the delay in samples of the maximum value of the impulse response, relative to the non-scattered/zero-delay component. In minimally scattered regimes, $L = 0$. In multiple scatter dominated regimes, $L > 0$. The parameter a_1 defines the rate of geometric decay of the impulse response after the peak, and represents the temporal spread of photon arrival times at the receiver. Low turbidities result in closely compacted photon arrival times (small a_1) while higher turbidities result in long multipath tails (large a_1).

C. Adaptive Determination of Channel Model Parameters

The channel model parameters can be determined adaptively, without using any *a priori* knowledge of the channel except its direct path length d. This is demonstrated next by convolving a simulated known training sequence $x(n)$ with the $h(n)$, the channel impulse responses derived from the experimentally measured channels from [6]. The training sequence is a 10^5-sample pseudo-random noise (PRN) on-off keying sequence with a nominally flat frequency spectrum from 0 to $f_s/2$. The received signal $d(n)$ is given according to Equation 1. To simulate a realistic scenario, a Gaussian noise signal is added such that the received signal $d(n)$ has a signal-to-noise (SNR) of 20 dB.

Both numerator parameters are found by calculating the cross-correlation $r_{xd}(k)$ of the received data, $d(n)$, with the known training sequence, $x(n)$. The correlation lag, $k = k_0 + k_e$, is the sum of the direct photon path between transmitter and receiver ($k_0 = d/(v/1.33)$ where d is range and $v/1.33$ is the speed of light in water), plus the average 'excess path' due to multiple scattering (k_e). The amplitude of $r_{xd}(k = k_0)$ is b_0, the zero-delay parameter of the filter model. The maximum-delay parameter, L, is the value $k_e = k - k_0$ at the maximum value of $r_{xd}(k)$. If $L \leq 1$, then the numerator of $\hat{H}(z)$ is fully known. If $L > 1$, then terms $[b_1 \ ... \ b_{L-1}]$ can be approximated by linearly interpolating between b_0 and b_L.

The denominator parameter a_1 can be found through the iterative process shown in Fig. 2. The training sequence is convolved with both the experimentally measured channel response (output $d(n)$), and the adaptive filter model of Eq. 2 (output $y(n)$). The difference between these outputs is the error $e(n)$. An error minimization algorithm iteratively updates a_1 (the numerator is already fully known from the cross-correlation steps listed above). For the $(k+1)^{th}$ iteration, the update equation of the algorithm is given by [8]:

$$\mathbf{c}(n+1) = \mathbf{c}(n) + \mu e(n)\mathbf{u}(n) \tag{3}$$

Here the filter coefficient vector is

$$\mathbf{c}(n) = \begin{bmatrix} b_0 & b_1 & ... & b_L & a_1(n) \end{bmatrix}^T$$

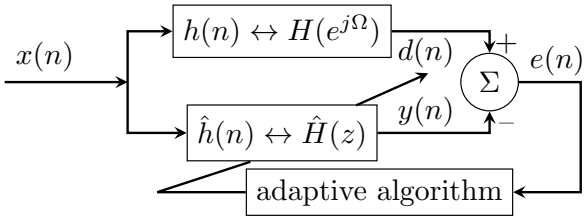

Fig. 2. Block diagram of adaptive channel identification. The upper arm of the channel equalizer $h(n)$) represents the water channel, while the bottom arm $\hat{h}(n)$ is the channel model filter, characterized by the three parameters b_0, L and a_1 (see text). The adaptive algorithm runs iteratively to minimize $e(n)$ such that $\hat{h}(n)$ models $h(n)$.

TABLE I
Parameters of Channel Model $\hat{h}(n) \leftrightarrow \hat{H}(z)$ Versus Attenuation Lengths *cd*

cd	b_0	L	a_1
0.2 - 9.2	1.00	0	0.00
11.8	1.00	0	0.12
14.4	1.00	0	0.58
16.7	0.54	1	0.49
19.8	0.24	1	0.62
23.7	0.07	2	0.51
28.8	0.05	2	0.62

the training sequence vector is

$$\mathbf{u}(n) = \begin{bmatrix} x(n) & x(n-1) & ... & x(n-L) & -y(n-1) \end{bmatrix}^T$$

the error is

$$e(n) = d(n) - \mathbf{u}^T(n)\mathbf{c}(n)$$

and μ is a user-controlled step size parameter. As $e(n)$ approaches zero, the adaptive filter $\hat{H}(z)$ becomes a good model for the water channel.

The described approach was used to generate IIR filter models for each of the experimentally measured impulse responses. Figure 3 shows the modeled responses overlaid with the experimental impulse responses for $cd > 11.8$. The good match of the modeled responses with the experimental responses corroborates the hypotheses that relatively simple few-parameter digital filter can be used to model the underwater optical channel, and that its parameters can be determined adaptively. Table I shows the parameter values calculated for each water turbidity. For $cd < 10$, no significant amount of dispersion was observed, so the measured impulse response was close to a delta function. For $10 < cd < 15$, both non-scattered and multiply scattered light contributes to the channel response. Here, $b_0 = 1$ and $L = 0$, but the a_1 values increase as turbidity increases. For $cd > 15$, multiply scattered light dominates. Here, a_1 increases with turbidity, and the impulse response peak shifts to the right, such that $b_0 < 1$ and $L > 0$.

III. Channel Equalization

Having modeled the channel, an equalization filter, $C(z)$ can be constructed and added at the receiver to mitigate the effects of multiple scattering. Ideally, the equalizer would be the inverse of the channel estimate, i.e. $C(z) = \hat{H}^{-1}(z)$, so that $C(z)$ would cancel the channel as much as possible. However, since $\hat{H}(z)$ has zeros in the numerator at high turbidity (when

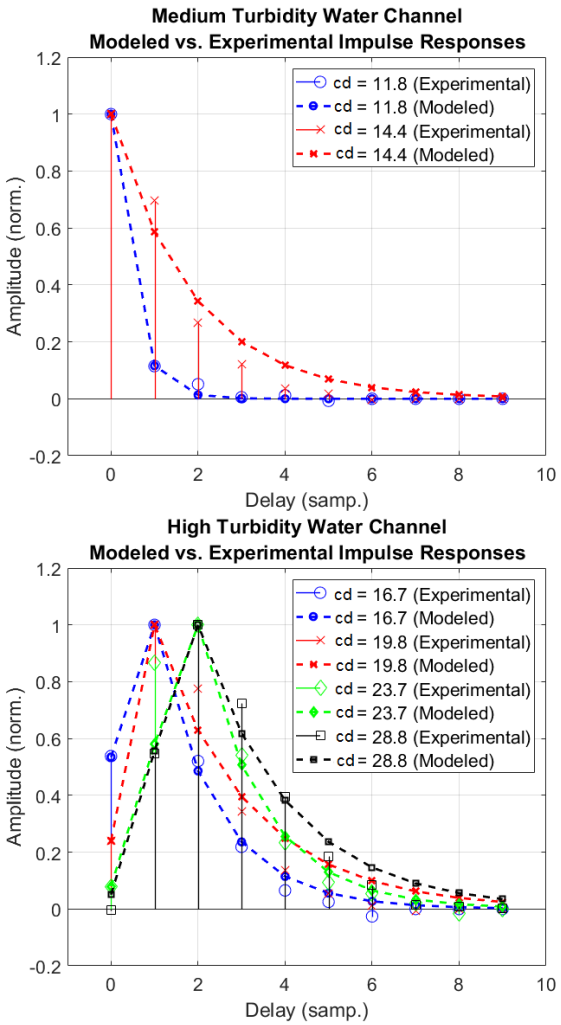

Fig. 3. Modeled vs. experimental impulse responses for medium- and high-turbidity water channels. The experimental impulse responses are the same as in Fig. 1. The modeled impulse responses are those associated with the channel model filters $\hat{h}(n)$, found by the channel identification process shown in Fig. 2.

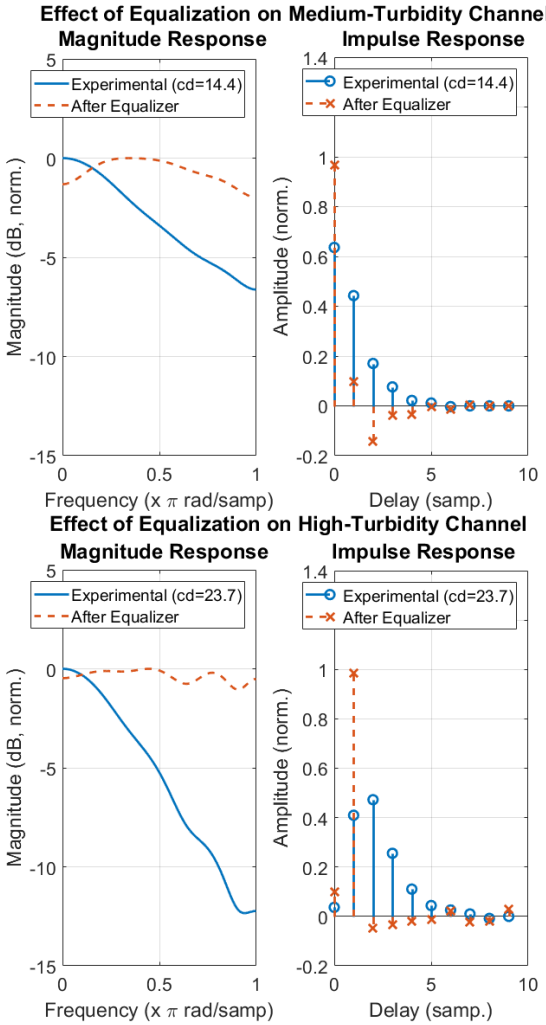

Fig. 4. Effect of equalization on channel response for example medium- and high-turbidity water channels. When an equalization filter is applied to the experimental channel, the magnitude response is flattened (top left, bottom left panels). The impulse response is sharpened (top right, bottom right panels) such that most of the energy is consolidated into one peak. Residual energy elsewhere in the impulse response is thought to be due to phase distortion in the equalizer.

L¿0), $C(z)$ will need to have poles to cancel $\hat{H}(z)$'s zeros, which may fall outside the unit circle on the z-plane. When this occurs, the poles of $C(z)$ must be mirrored in the unit circle from the corresponding zeros in $\hat{H}(z)$. This ensures the stability of $C(z)$, and provides an inversion of $\hat{H}(z)$'s magnitude response, but it can introduce a distortion in the phase response.

Figure 4 illustrates the effect of the equalization on channels of $cd = 14.4$ and $cd = 23.7$. The experimentally measured magnitude responses (in blue) for both channels are non-flat, with the channel gain decaying by up to 12 dB in the $cd = 23.7$ case over the frequency band from 0 to $f_s/2$. When the equalizer is applied, the magnitude response is flattened significantly, varying by less than 2 dB across the spectrum in both cases. Similarly, the channel impulse responses show a de-spreading of energy from several samples in the experimental impulse response, into a single sample in the equalized impulse response. This suggests that the equalized channel should see a significant reduction in ISI for high-speed communication links. The remaining variation in the magnitude response is thought to be due to slight inaccuracies in calculating the b_0 and a_1 parameters, since they were calculated in the presence of additive noise. Residual energy spreading in the time domain is thought to be due both to parameter inaccuracy and also to the phase response distortion from unit-circle-mirrored pole placements as discussed above.

IV. Simulated Data Transmission through Turbid Water

A. Simulation Method

Having experimentally measured the frequency response of the underwater optical channel, confirming that these responses can be modeled using a simple digital adaptive filter, and demonstrated that channel equalizing filters can be created from those models, proof-of-concept communication

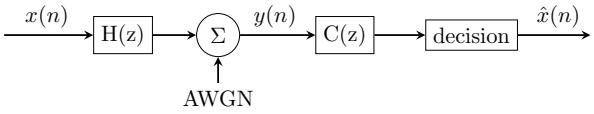

Fig. 5. Block diagram of simulation. A random binary data stream $x(n)$ passes through the experimental channel $H(z)$ before additive white Gaussian noise (AWGN) is added to it to control the signal to noise ratio (SNR). The channel equalizer filter $C(z)$ is applied to undo the effects of the channel $H(z)$. A thresholding decision block then attempts to recover $x(n)$, yielding $\hat{x}(n)$. The bit error rate (BER) is calculated between $x(n)$ and $\hat{x}(n)$ at various SNR values.

simulations were performed to assess the possible performance improvement gained by channel equalization.

Figure 5 shows the simulation approach. A random binary data stream of $N_b = 10^6$ bits is generated, and is transmitted as a unipolar OOK signal $x(n)$ of amplitude 0 or 1. This signal is convolved with the experimentally measured channel impulse responses, and Gaussian noise is added to achieve the desired SNR which was varied from 0-40 dB. The equalization filter is applied, and the receiver then uses a simple decision block with a threshold of amplitude 0.5 to decode the signal, yielding the received sequence $\hat{x}(n)$.

Simulations were performed for each experimentally measured channel, both with and without the equalization filter $C(z)$, at data rates of 1.1 Gbps, 550 Mbps, 367 Mbps, and 275 Mbps. The bit error rate (BER) is calculated by tabulating the number of errors N_e in the received $\hat{x}(n)$ when it is compared to the transmitted number of bits N_b transmitted in $x(n)$, eg. $BER = N_e/N_b$.

B. Simulation Results

Figure 6 shows the equalized and unequalized BER versus SNR at $cd = 14.4$, 19.8, and 28.8, for each data rate. The figure illustrates the improvement in communication performance given a fixed environment (either range or turbidity). The unequalized responses show that for a given SNR, the BER increases with increasing data rate. This is consistent with the low-pass nature of the channel response as reported by the experimental measurements in [4], [5], [6]. Applying the channel equalizer improves link performance by providing a similar BER than the unequalized channel, but at a lower SNR. The improvement is dramatic in some instances. For example, at $cd = 19.8$, channel equalizations allows the 367 Mbps, 550 Mbps, and 1.1 Gbps links to be closed whereas the unequalized link is infeasible (ie BER≈ 0.5).

Figure 7 presents the SNR required for BER=10^{-5} as a function of water turbidity (cd) at each data rate (this BER is arbitrarily chosen as an 'acceptable' rate for realistic operation). This illustrates the potential of equalization to extend acceptable link performance with increasing range or turbidity. The equalized data curve 1.1 Gbps exhibits a break at $cd \approx 17$, which despite channel equalization did not result in a closed link. It is believed this is due to distortions in the phase response of the equalizer at this turbidity, as described previously.

The results in the previous two figures are summarized quantitatively in Table II, which shows the BER improvement

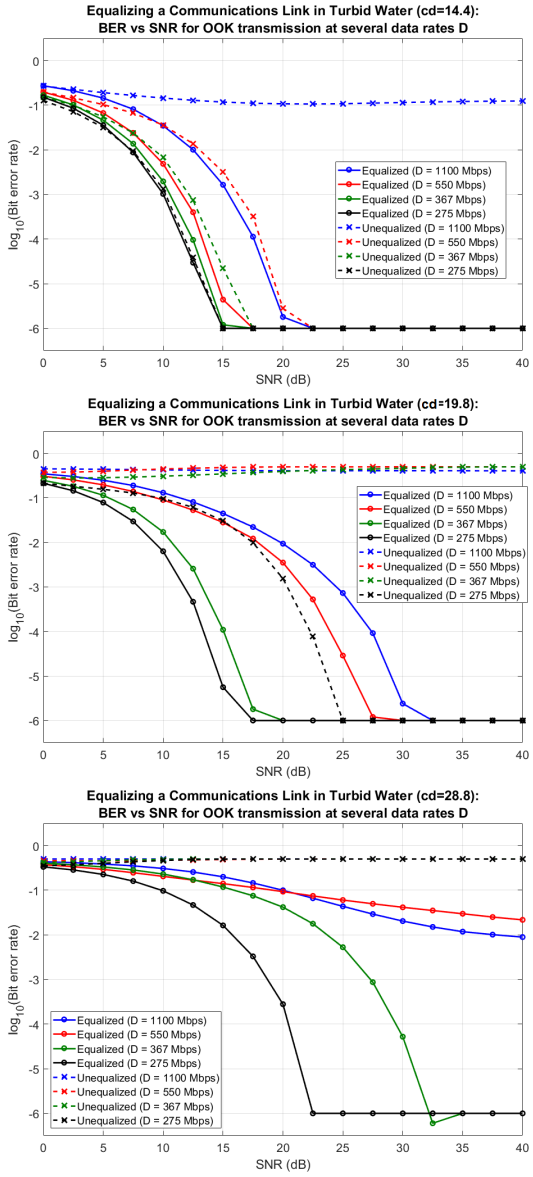

Fig. 6. BER vs SNR in multiple scattering scenarios, both with and without channel equalization. In a medium-turbidity example (top panel), the unequalized link fails for the maximum data rate, but equalization allows this rate to be used. When turbidity is increased (middle), an unequalized link is established only at the lowest data rate, but equalization allows use of all data rates. At the highest turbidity (bottom), only the equalized, low-data rate links are successful.

between equalized and unequalized channels for 1.1 Gbps and 275 Mbps links in multiple scattering environments. The table assumes a 20 dB SNR threshold is required at the receiver, and illustrates the trends in performance improvement in multiple scattering environments when using a channel equalizer.

All together, the simulations show that equalization can either improve BER at a given range/turbidity, or, extend the same performance over longer ranges/turbidities. As our equalizers were synthesized using laboratory measurements of channel dispersion made under a specific set of variables, it is important to recognize that the results are only illustrative of the potential of channel equalizers for underwater optical communications, rather than a definitive or theoretical performance

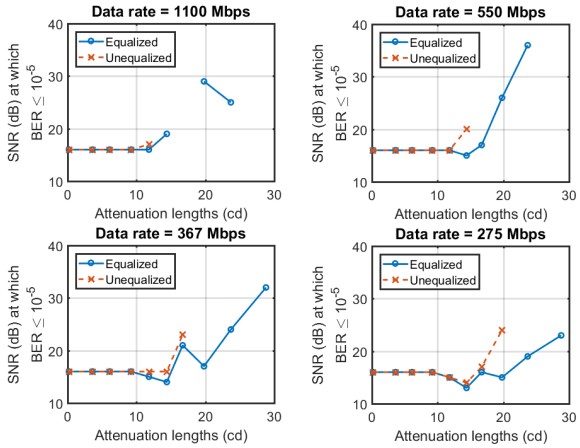

Fig. 7. SNR required to achieve a BER of 10^{-5}, as a function of attenuation length *cd*. At high data rates of 1100 Mbps and 550 Mbps (top panels), equalization allows a link to be established for some, but not all, high attenuation length scenarios. At lower data rates (bottom panels), equalization allows the link to be established at all tested attenuation lengths. For all data rates, the SNR required to achieve the desired BER is typically reduced for medium- and high-turbidity cases.

TABLE II
BER IMPROVEMENT USING CHANNEL EQUALIZATION FOR 1.1 GBPS AND 275 MBPS LINKS IN MULTIPLE SCATTERING ENVIRONMENTS. SNR=20 DB IS ASSUMED.

	1.1 Gbps		**275 Mbps**	
cd	*unequalized*	*equalized*	*unequalized*	*equalized*
11.8	$< 10^{-6}$	$< 10^{-6}$	$< 10^{-6}$	$< 10^{-6}$
14.4	10^{-1}	10^{-6}	$< 10^{-6}$	$< 10^{-6}$
19.8	$10^{-0.4}$	$10^{-2.0}$	$10^{-2.8}$	$< 10^{-6}$
28.8	$10^{-0.3}$	$10^{-1.0}$	$10^{-0.3}$	$10^{-3.5}$

limit. In practice, the quantitative impact of the equalizer (and of channel dispersion itself), will be a function of not only water turbidity, but also link range, particles size and shape (eg the scattering phase function), receiver aperture and field of view, transmitter beam divergence (line-of-sight or diffuse), and link geometry, just to name a few. Finally, the results show that at low and moderate turbidities ($cd < 10$), there was little benefit in using channel equalization. This is consistent with the experimental channel measurements we used from [6], which showed dispersion-free transmission in the magnitude and phase responses at these bandwidths over the same number of attenuation lengths.

V. CONCLUSION

Well-behaved trends in the impulse responses of previously measured underwater optical channels are observed, namely, a delay in the average arrival time of transmitted light pulses and a temporal spreading of their energy. This behavior was leveraged to model measured channel responses with a simple 3-parameter IIR filter model whose three parameters can be found without *a priori* knowledge of the water channel. Equalization filters were derived from the channel models, and simulations illustrated their ability to mitigate the temporal dispersion present due to multiple scattering. The resulting reduction in ISI allows for improved BER at a given range/turbidity, or, the ability to achieve a sufficient BER at longer attenuation lengths.

To develop the digital filter channel models in this study, we leveraged experimental laboratory measurements of the channel frequency response that had been previously reported. These previously acquired responses were used to simulate the transmission of a training sequence through an unknown underwater optical channel in order to demonstrate the appropriateness of the proposed digital filter channel model as well as the ability to determine the filter parameters adaptively. Obviously, it is not reasonable to posses prior empirical measurements of the communications channel in real-world situations. Rather, the model parameters would be determined by transmitting the training sequence through the underwater channel directly. Future work will demonstrate this via experimental implementation of channel adaptation and equalization with real data in laboratory test tanks.

FUNDING

This work was supported by the Office of Naval Research's Naval Research Enterprise Internship Program (NREIP).

ACKNOWLEDGMENTS

We thank Dr. Linda Mullen for helpful discussions, and Alan Laux for assistance with the experimental channel frequency response measurements.

REFERENCES

[1] J. Xu, A. Lin, Y. Song, M. Kon, F. Qu, J. Han, W. Jia, and N. Deng. "Underwater laser communication using an OFDM modulated 520-nm laser diode," IEEE Photon. Techol. Lett. **28**(20), 2133–2136 (2016).
[2] N. Farr, J. Ware, and C. Pontbriand. "Demonstration of wireless data harvesting from a subsea node using a ship of opportunity," in *Proceedings of Oceans - San Diego* (IEEE, 2013).
[3] M. Doniec, A. Xu, and D. Rus. "Robust real-time underwater digital video streaming using optical communication," in *Proceedings of IEEE International Conference on Robotics and Automation* (IEEE, 2013).
[4] B. Cochenour, L. Mullen, and J. Muth. "Temporal response of underwater optical channel for high-bandwidth wireless laser communications," IEEE Journal of Oceanic Engineering, **38**(4), 730–742 (2013).
[5] B. Cochenour, A. Laux, and L. Mullen, "Temporal dispersion in underwater laser communication links: Closing the loop between model and experiment," in *Proceedings of IEEE Underwater Communications and Networking Conference* (IEEE, 2016).
[6] B. Cochenour, K. Dunn, A. Laux, and L. Mullen. "Experimental measurements of the magnitude and phase response in turbid underwater optical channels," Applied Optics **56**(14), 4019–4024 (2017).
[7] H. Lu, C. Li, H. Lin, W. Tsai, C. Chu, B. Chen, and C. Wu. "An 8m/9.6 Gbps Underwater Wireless Optical Communication System," IEEE Photon. J. **8**(5), (2016).
[8] D. Manolakis, V. Ingle, and S. Kogon. *Statistical and Adaptive Signal Processing,* (McGraw Hill, 2000).
[9] D. DeFatta, J. Lucas, and W. Hodgkiss. *Digital Signal Processing: A System Design Approach,* (Wiley, 1998).